

## Fabrication and Characterization of Sulfonated Polysulfone Membrane with Different Thicknesses for Proton Exchange Membrane Fuel Cell

İrem Tanış<sup>1\*</sup> , Turan Alp Arslan<sup>2</sup> , Tolga Kocakulak<sup>3,4</sup> , Gülşen Taşkın<sup>5</sup> , Tuğba Tabanlıgil Calam<sup>5</sup>   
Hamit Solmaz<sup>1,6</sup> 

<sup>1</sup> Automotive Engineering Department, Faculty of Technology, Gazi University, Ankara, 06500, Turkey

<sup>2</sup> Automotive Engineering Department, Faculty of Technology, Afyon Kocatepe University, Afyonkarahisar, 03200, Turkey

<sup>3</sup> Automotive Engineering Department, Graduate School of Natural and Applied Sciences, Gazi University, Ankara, 06500, Turkey

<sup>4</sup> Vocational High School of Technical Sciences, Burdur Mehmet Akif Ersoy University, Burdur, 15100, Turkey

<sup>5</sup> Technical Sciences Vocational High School, Gazi University, Ankara, 06374, Turkey

<sup>6</sup> Mechanical Engineering Department, Faculty of Engineering, University of Alberta, T6G 1H9, Canada

### ABSTRACT

Membranes play a critical role in the performance of proton exchange membrane fuel cells. Membrane thicknesses have positive and negative effects on the characteristics of proton exchange membranes. In this study, sulfonated polysulfone (SPSf) polymer-based membranes with thicknesses of 50  $\mu\text{m}$ , 100  $\mu\text{m}$ , and 150  $\mu\text{m}$  were fabricated, and their characteristic properties were investigated. Water uptake capacity, swelling ratio, proton conductivity, contact angle, chemical stability, and mechanical strength tests were carried out on the membranes. Maximum water uptake capacity and swelling ratio were 45.81% and 13.1% for 100  $\mu\text{m}$  SPSf membrane, respectively. The results of contact angle analysis proved that all synthesized membranes were hydrophilic. Proton conductivity values were measured at different temperatures and solution environments. Significant decreases in resistance values and increases in proton conductivity were observed with decreasing membrane thickness. The increase in temperature and acid in the measurement conditions caused an increase in the proton conductivity value. The highest proton conductivity value was obtained as 0.1971 S/cm in 65 °C and 1 mM hydrochloric acid (HCl) aqueous solution environment in 50  $\mu\text{m}$  SPSf membrane. It was determined that the chemical stability and mechanical strength decreased with the decrease in membrane thickness but remained within the appropriate limits.

**Keywords:** Fuel Cell; Membrane; Proton Exchange Membrane; Sulfonated Polysulfone; Thickness

#### History

Received: 09.03.2024

Accepted: 18.07.2024

#### Author Contacts

\*Corresponding Author

e-mail addresses: [tanisirem430@gmail.com](mailto:tanisirem430@gmail.com), [talparslan@aku.edu.tr](mailto:talparslan@aku.edu.tr), [kocakulak@mehmetakif.edu.tr](mailto:kocakulak@mehmetakif.edu.tr), [gulsentaskin@gazi.edu.tr](mailto:gulsentaskin@gazi.edu.tr), [ttabanligil@gazi.edu.tr](mailto:ttabanligil@gazi.edu.tr), [hsolmaz@gazi.edu.tr](mailto:hsolmaz@gazi.edu.tr)

#### How to cite this paper:

Tanış, İ., Arslan, T.A., Kocakulak, T., Taşkın, G., Calam, T.T., Solmaz, H. (2024). Fabrication and Characterisation of Sulfonated Polysulfone Membrane with Different Thicknesses for Proton Exchange Membrane Fuel Cell. *Engineering Perspective*, 4 (3), 100-107. <http://dx.doi.org/10.29228/eng.pers.77899>

### 1. Introduction

The world's need for energy is increasing rapidly due to the increase in the human population and the development of industry and technology. This need, which is increasing day by day, has caused wars in the world since the past and adversely affects environmental conditions [1,2]. There is no doubt that fossil fuels such as coal, oil, and natural gas cause environmental pollution, acid rain, global warming, and climate change during energy production. This situation has caused the scientific world to intensify research on alternative and renewable energy sources [3,4].

Renewable energy sources that are environmentally friendly compared to fossil energy sources can be listed as solar, hydroelectric, wind, geothermal, wave, and biomass energy [5-7]. In addition to these energy sources, researches indicate that hydrogen energy is the renewable energy of the future. Since water vapor is released from hydrogen combustion reactions, the environment is not harmed [8]. The technology that uses hydrogen energy most efficiently and economically is fuel cell technology [9].

Fuel cells have advantages such as almost zero emission, easy refueling, noiseless operation, and lightweight. With these advantages, they can be used in many vehicle types where internal combustion

engines and batteries are used. Despite these advantages, they also have disadvantages, such as inefficient storage, transport, and distribution of fuels and high production costs.

Today, fuel cells are classified according to electrolyte type, fuel type, membrane structure material, catalyst material, power density, operating temperature, and efficiency. Fuel cells are divided into six classes according to electrolyte type: alkaline, proton exchange membrane, direct methanol, phosphoric acid, molten carbonate, and solid oxide fuel cells [10-12]. Proton exchange membrane fuel cell (PEMFC) has primary advantages over other fuel types, such as no risk of electrolyte leakage, short warm-up time, and high specific power. Therefore, the PEM fuel cell is one of the most preferred fuel cells today [13,14]. Proton exchange membrane (PEM) fuel cell is a type of fuel cell that directly and efficiently converts the chemical energy stored in the fuel into electrical energy, providing high power and energy at low operating temperatures.

Fuel cells consist of gas flow plate, gas diffusion layer, catalyst layer, membrane, current collector plate, and sealing components [15]. The gas flow plate ensures that the fluids in the fuel cell are evenly and effectively distributed on the electrode surface. It also helps to remove the heat generated during electrochemical reactions from the cell. The gas diffusion layer ensures that hydrogen and oxygen gases are evenly and continuously delivered to the catalyst layer. In addition to this task, it helps to transmit the electricity generated in the catalyst to the gas flow plate and from there to the external circuit. In the cell, the catalyst layer is where reduction and oxidation reactions occur. It separates and combines reactive gases (hydrogen and oxygen). Membranes transmit protons formed by the breakdown of hydrogen on the anode side to the cathode side. Since it is not permeable to electrons, it causes electrons to flow through the external circuit and produces electrical energy [16,17].

In order to expand the usage area of fuel cells further, cost, efficiency, and performance values should be improved. For this reason, researchers have conducted various studies to determine the effects of thickness variation of the membrane, which is one of the critical components of the fuel cell. For example, Lufrano et al. synthesized membranes with different sulfonation degrees (57% and 66%) and thicknesses (70, 120, and 150  $\mu\text{m}$ ) for direct methanol fuel cell (DMFC) and characterized them in terms of methanol/water uptake, proton conductivity, and fuel cell performances at room temperature in passive mode. They obtained the best performance with 70  $\mu\text{m}$  SPSf-2 membrane (66% sulfonation degree) [18]. Zhang et al. synthesized SPSf membranes with various sulfonation degrees (62%, 67%, 76%, and 91%) and thicknesses (76, 80, 79, and 76  $\mu\text{m}$ ). They characterized the physicochemical properties, ion permeability, and vanadium redox flow battery (VRFB) performance of the obtained SPSf membranes. As a result of the study, the SPSf-62 membrane with 62% sulfonation degree showed the best performance. This membrane exhibited better ion permeability and cycle stability than Nafion 117 [19]. Zhao et al. studied the effect of Nafion (117, 115, and 112) thickness on DMFC. With Nafion 117, 115, and 112 membranes with thicknesses of 174, 125, and 50  $\mu\text{m}$ , they found that a thicker membrane showed higher fuel efficiency. However, the fuel cell performance varied with different operating conditions, such as methanol concentration and current density [20].

As a result of the literature search, there is quite a limited number of studies investigating the effect of thickness on the characteristic

properties of SPSf-based polymer membranes produced for use in PEM fuel cells. For this reason, in this study, SPSf membranes with thicknesses of 50  $\mu\text{m}$ , 100  $\mu\text{m}$ , and 150  $\mu\text{m}$  were produced and characterized for proton exchange membrane fuel cells. During the characterization process, water uptake capacity, swelling ratio, proton conductivity, contact angle, chemical stability, and mechanical strength tests were carried out, and the effects of thickness on membrane performance were investigated.

## 2. Materials and Methods

In this study, fabrication and characterization of SPSf polymer-based PEM fuel cell membranes with 50  $\mu\text{m}$ , 100  $\mu\text{m}$ , and 150  $\mu\text{m}$  thicknesses were carried out. Water uptake capacity, swelling ratio, proton conductivity, contact angle, chemical stability, and mechanical strength tests were applied to the fabricated membranes. As a result of the characterization processes, the physical, chemical, and electrochemical performances of membranes with different thicknesses were investigated.

### 2.1. Sulfonation process

Pure polysulfone (PSf) pellets (Sigma-Aldrich), chloroform (Sigma-Aldrich), and sulfuric acid ( $\text{H}_2\text{SO}_4$ , Merck) were used for the sulfonation of PSf polymer. Firstly, 10 g PSf was weighed and dissolved in 100 ml chloroform with the help of a magnetic stirrer. The sulfonation process was started by slowly adding 3 ml  $\text{H}_2\text{SO}_4$  to the stirring solution. The stirring process was continued for 6 hours, which is the sulfonation duration. In order to complete the sulfonation, the prepared solution was transferred to an ice water bath, and the polymers were precipitated [21]. The precipitated polymers were washed with distilled water until neutralized. Ohaus brand AB23PH-F model digital pH meter was used to measure the pH value of the solution. After washing, SPSf polymers were dried in an oven at 80  $^\circ\text{C}$  for 48 hours [22].

### 2.2. Synthesis of membranes

In the study, membranes with thicknesses of 50  $\mu\text{m}$ , 100  $\mu\text{m}$ , and 150  $\mu\text{m}$  were produced. For each membrane sample, 2 g of SPSf polymer was weighed using a precision balance. After weighing, SPSf was dissolved with 5 mL dichloromethane (DCM, Aklar Kimya). Membrane castings were carried out using the Biuged Instruments brand BGD-219 model automatic film applicator. SPSf membranes of the specified thicknesses were left to dry at room temperature after casting. Images of the membrane samples are shown in Figure 1.

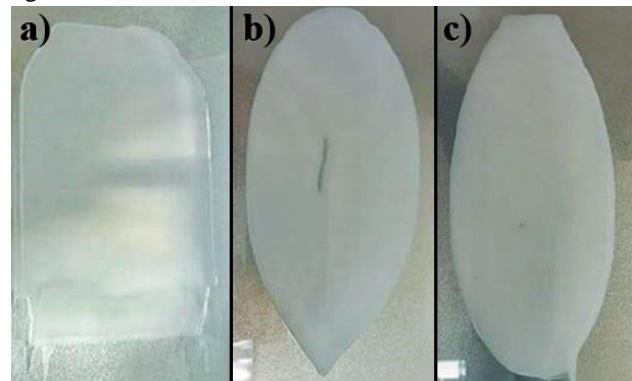


Figure 1. SPSf membrane samples: a) 50  $\mu\text{m}$ , b) 100  $\mu\text{m}$ , and c) 150  $\mu\text{m}$

### 2.3. Water uptake capacity and swelling ratio analyses

Water uptake capacity is the most important of the properties affecting proton conductivity in membranes. Membranes with high water uptake capacity are needed for high proton conductivity values [23]. However, with the increase in water uptake capacity, an increase in the swelling properties of membranes can also be observed. With swelling, the membrane thickness increases and creates proton conduction resistance [24]. Therefore, it is desired to keep the membrane water uptake at an optimum level [25]. Membrane water uptake capacity and swelling ratio values can be determined by experimental methods.

To determine water uptake capacity (WU) and swelling ratio (SR), SPSf membrane samples were dried in an oven at 70 °C for 24 h. Mass and dimensional measurements of the dried membrane samples were made. Afterwards, the membranes were kept in deionized water for 24 h. After the membranes were dewatered, the mass and dimensional measurements of the samples were carried out again. Using the measured masses and dimensions of dry and wet membranes, the water uptake capacity was calculated by Eq. (1), and the swelling ratio was calculated by Eq. (2) [26,27].

$$WU (\%) = \frac{m_{wet} - m_{dry}}{m_{dry}} \cdot 100 \quad (1)$$

$$SR (\%) = \frac{V_{wet} - V_{dry}}{V_{dry}} \cdot 100 \quad (2)$$

Where  $m_{wet}$  is wet mass,  $m_{dry}$  is dry mass,  $V_{wet}$  is wet volume and  $V_{dry}$  is dry volume.

### 2.4. Measurement of proton conductivity

Proton conductivity ( $\sigma$ ) is the most important criterion for the performance and efficiency of proton exchange membrane fuel cells. In order to increase the proton conductivity in proton exchange membrane fuel cells, the membrane resistance should be low as well as the appropriate operating temperature and humidity [28]. The proton conductivity of membranes can be measured using the Electrochemical Impedance Spectroscopy (EIS) technique with the help of 2, 3, or 4 probe cells and potentiostat [29-31]. The 4-probe measurement method is widely preferred thanks to its better measurement accuracy [32].

In this study, proton conductivities were measured in two different environments. The first was deionized water at 25 °C; the second was 1 mM hydrochloric acid (HCl) and aqueous solution at 65 °C. The proton conductivity measurement process and the measurement cell with four probes are shown in Figure 2.

Ivium brand Compartment model electrochemical workstation was used in the measurements. The measurements were performed at a frequency range of 1 Hz-100 kHz, and an amplitude of 0.1 V. IviumSoft software was used to create equivalent electrical circuit models of SPSf membranes and to determine the resistance values. Proton conductivities of the membranes were calculated with Eq. (3) by utilizing the measured membrane resistance and sample dimensions [33].

$$\sigma = \frac{L}{R \cdot w \cdot t} \quad (3)$$

Where L is the distance between the two internal electrodes, R is

the membrane resistance, w is the membrane width, and t is the membrane thickness.

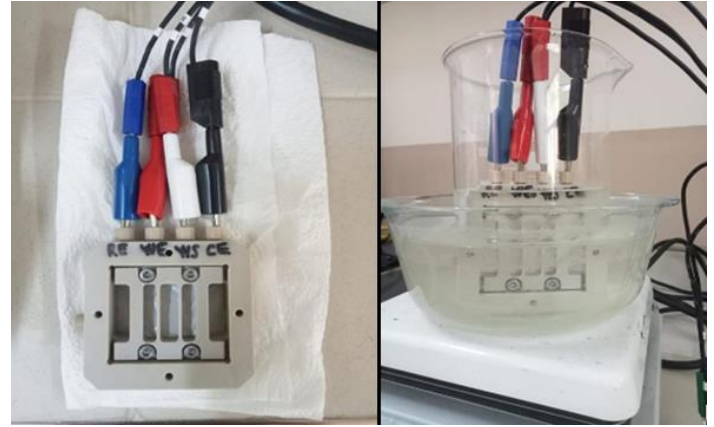


Figure 2. Four-probe cell and measurement process

### 2.5. Contact angle analysis

Wetting is defined as the ability of the liquid to maintain the contact of the liquid on the solid due to the effect of adhesion forces at the solid-liquid interface during the contact of liquid and solid surfaces. The indicator of the wettability of a solid object with a liquid is the contact angle between the liquid drop and the solid surface [34]. The contact angle can vary between 0° and 180°. A contact angle smaller than 90° means the material is hydrophilic, and a larger contact angle means the material is hydrophobic [35]. Contact angle analyses are performed to evaluate membranes' hydrophilic and hydrophobic characteristics [36].

Contact angles of SPSf membranes of different thicknesses were measured at room temperature using the sessile drop method and deionized water. Biolin Scientific brand Attension Theta model optical contact angle measuring device was used in the measurements.

### 2.6. Fenton chemical stability test

The degradation of proton exchange membranes is caused by chemical, electrochemical, mechanical, and thermal reasons. Degradation of PEMs can significantly reduce fuel cell efficiency [37,38]. The Fenton test is widely preferred for investigating the chemical stability of PEM fuel cell membranes [39].

To determine the chemical stability of SPSf membranes, a Fenton reagent solution was prepared using iron II sulfate ( $\text{FeSO}_4$ , Aklar Kimya), hydrogen peroxide (50%,  $\text{H}_2\text{O}_2$ , Aklar Kimya), and deionized water. In the first stage of the Fenton test, membranes of different thicknesses were kept in an oven at 70°C for 24 hours and weighed. Then, the dry membranes were kept in 3%  $\text{H}_2\text{O}_2$ , 4 ppm  $\text{Fe}^{+2}$  aqueous solution for 1 day and 7 days. At the end of this period, the membranes were dried again in the oven under the same conditions, and their final masses were recorded. The weight loss (WL) resulting from the Fenton reaction was calculated by Eq. (4) using the measured masses of the membranes.

$$WL (\%) = \frac{m_{initial} - m_{end}}{m_{initial}} \cdot 100 \quad (4)$$

Where  $m_{initial}$  is the initial weight of the membranes after drying and  $m_{end}$  is the final weight after the Fenton reaction.

## 2.7. Mechanical strength test

The membrane can be defined as the backbone of the membrane-electrode assembly [40]. Mechanical strength tests are aimed to determine Young's modulus, tensile stress, and elongation at break values of membranes.

TIRA Test brand 2710 model tensile tester was used in mechanical strength tests of SPSf membranes. For mechanical strength tests, membranes of different thicknesses were cut to the specific dimensions, and tensile tests were carried out at room temperature at 2 mm/min speed. Elongation ( $\epsilon$ ), elongation at break (EB), Young's modulus (E), and tensile strength ( $\sigma_t$ ) values were calculated by Eq. (5), Eq. (6), Eq. (7), and Eq. (8), respectively.

$$\epsilon = \frac{\Delta L}{L} \quad (5)$$

$$EB (\%) = \frac{\Delta L}{L} \cdot 100 \quad (6)$$

$$E = \frac{\sigma}{\epsilon} \quad (7)$$

$$\sigma_t = \frac{F_{max}}{A_i} \quad (8)$$

In the equations,  $\Delta L$  is the change in the sample length,  $L$  is the initial length of the sample,  $F_{max}$  is the maximum tensile force applied to the sample, and  $A_i$  is the initial cross-sectional area of the sample.

## 3. Results and Discussions

In the study, the water uptake capacity, swelling ratio, proton conductivity, weight loss as a result of the Fenton reaction, tensile stress, Young's modulus, and elongation at break values of SPSf polymer-based proton exchange membranes with different thicknesses were characterized, and the effects of changes in thickness on membrane performance were investigated.

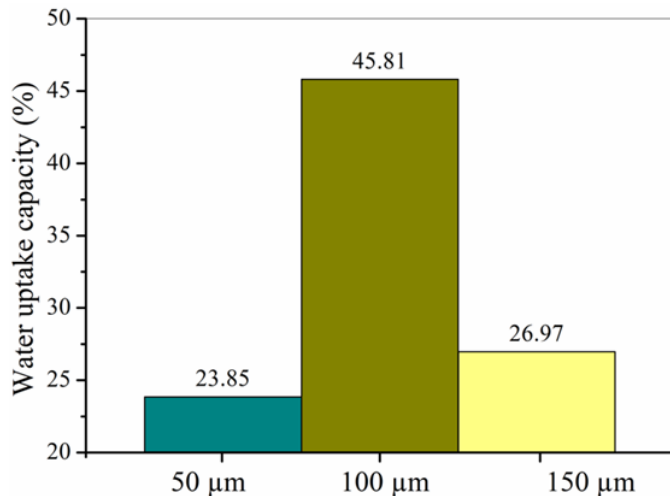


Figure 3. Water uptake capacity of SPSf membranes

### 3.1. Water uptake capacity

Water uptake capacity is one of the most critical parameters that trigger the proton conductivity of PEM fuel cell membranes. The water uptake properties of PEMs may vary depending on their thickness. The water uptake capacity values of the synthesized SPSf

membranes are shown in Figure 3. The water uptake capacities of the membranes with 50  $\mu\text{m}$ , 100  $\mu\text{m}$ , and 150  $\mu\text{m}$  thicknesses were determined as 23.85%, 45.81%, and 26.97%, respectively. The highest water uptake capacity value was obtained in the membrane with 100  $\mu\text{m}$  thickness.

### 3.2. Swelling ratio

It is desired that the membranes have a high water uptake capacity but a low swelling ratio. The reason for this is that the stresses due to swelling negatively affect the mechanical strength of the membrane, and the increase in thickness makes proton conductivity difficult. Swelling ratios for SPSf membranes with different thicknesses are presented in Figure 4. The swelling ratios for membranes with 50  $\mu\text{m}$ , 100  $\mu\text{m}$ , and 150  $\mu\text{m}$  thicknesses were obtained as 4.6%, 13.1%, and 3.5%, respectively. The high water uptake capacity in the 100  $\mu\text{m}$  membrane resulted in a high swelling ratio.

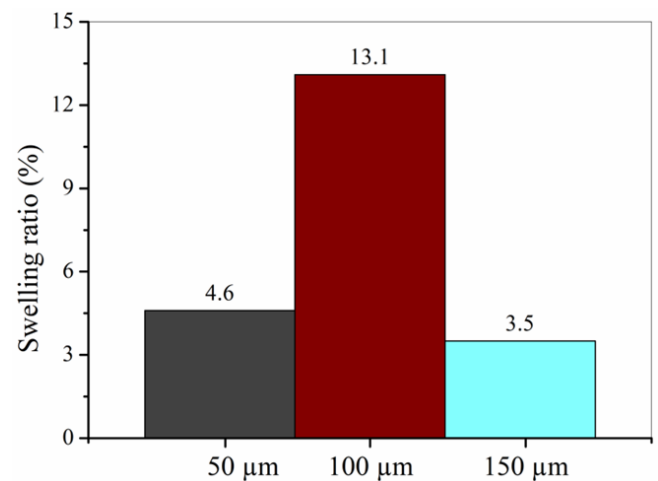


Figure 4. Swelling ratio of SPSf membranes

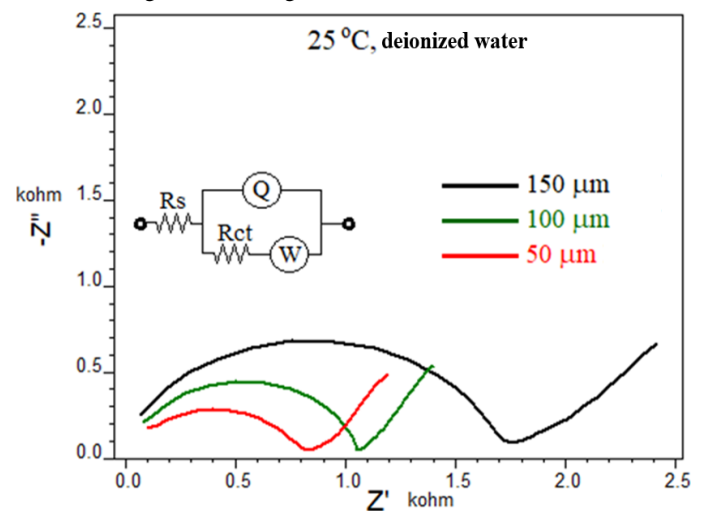


Figure 5. Nyquist plots of SPSf membranes (25 °C and deionized water)

### 3.3. Proton conductivity

Proton conductivity is one of the most important characteristics of PEM fuel cells. Membrane resistance directly affects proton conductivity. The Nyquist plot of membranes with different thicknesses at 25 °C and in deionized water environment is shown in Figure 5. A

significant increase in resistance values occurred with the increase in the thickness of SPSf membranes.

The Nyquist graph of SPSf membranes created at 65 °C temperature and 1 mM HCl aqueous solution environment is shown in Figure 6. Similar to the deionized water environment, a regular decrease in the resistance value occurred here as the membrane thickness decreased. At the same time, thanks to the increasing temperature and acid environment, the resistance values resulted in a lower level than those of the deionized water environment.

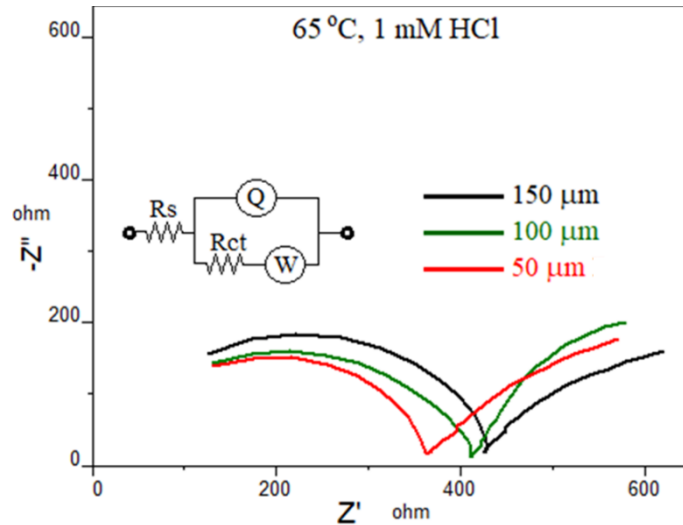


Figure 6. Nyquist plots of SPSf membranes (65 °C and 1 mM HCl)

The resistance values obtained in different measurement environments of SPSf membranes with different thicknesses are shown in Table 1, and the proton conductivity results calculated with these resistance values and dimensional parameters are shown in Table 2.

Table 1. Resistance values of SPSf membranes

Measurement conditions	Units	Membrane thickness (μm)		
	μm	50	100	150
25 °C, deionized water	kohm	798.9	1038	172.5
65 °C, 1 mM HCl	kohm	277.6	313.4	396

Table 2. Proton conductivity values of SPSf membranes

Measurement conditions	Units	Membrane thickness (μm)		
	μm	50	100	150
25 °C, deionized water	S/cm	0.0684	0.0205	0.0108
65 °C, 1 mM HCl	S/cm	0.1971	0.0613	0.0472

When the obtained results were examined, the highest proton conductivity in both environments was in the 50 μm SPSf membrane, while the lowest proton conductivity was in the 150 μm membrane. As the thickness of the SPSf membrane increased, a decrease in proton conductivity was observed. SPSf membranes showed higher proton conductivity in 65 °C, 1 mM HCl aqueous solution. One reason is that high temperature increases the activation energy and enables faster movement of protons. The second reason is that HCl opens proton carrier paths in the membrane [41]. As a result of impedance analysis, the highest proton conductivity value was measured as 0.1971

S/cm in 50 μm SPSf membrane in 65 °C and 1 mM HCl aqueous solution environment.

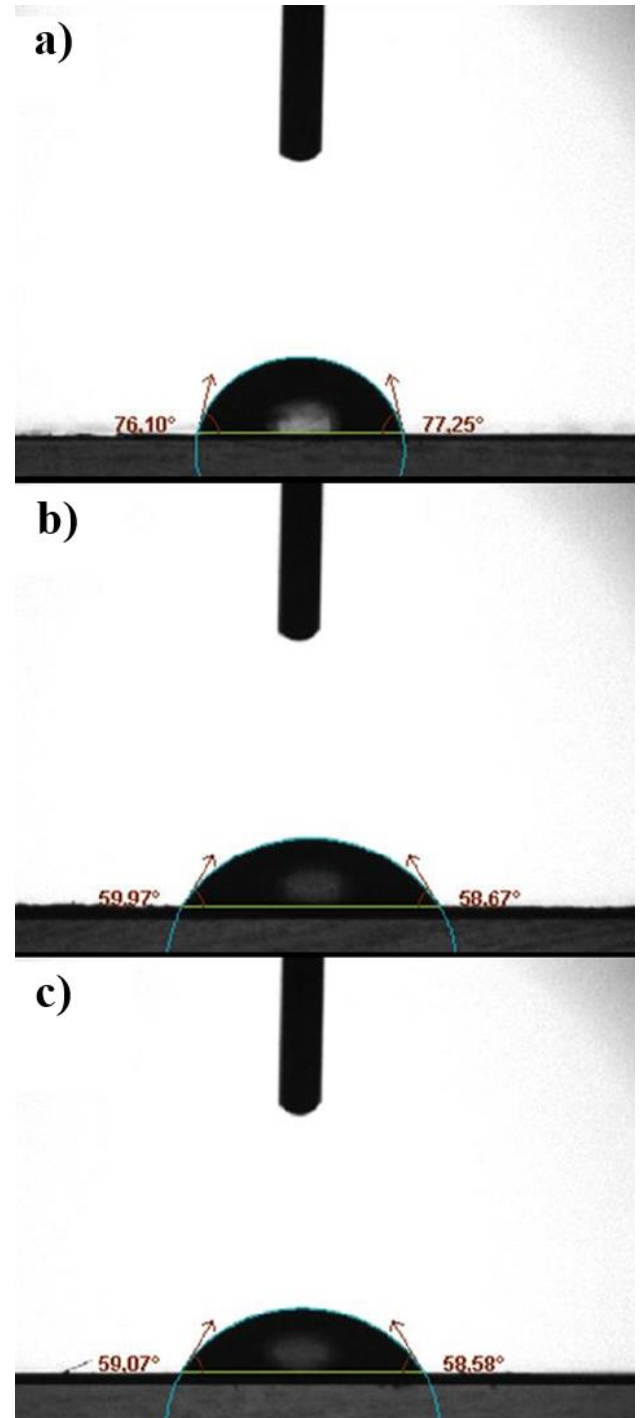


Figure 7. Contact angle images of SPSf membranes

### 3.4. Contact angle

Contact angle analyses were performed to evaluate the hydrophilic and hydrophobic characteristics of SPSf membranes produced with different thicknesses. Contact angle images of SPSf membranes are shown in Figure 7, and the average values of contact angle measurements are shown in Figure 8. The average contact angle values of SPSf membranes with thicknesses of 50 μm, 100 μm, and 150 μm were measured as 76.67°, 59.32°, and 58.83°, respectively. After the

analysis, it was concluded that all synthesized membranes were hydrophilic.

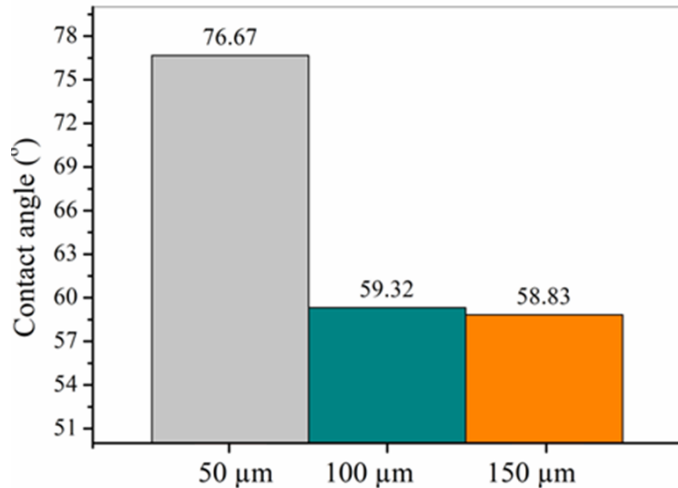


Figure 8. Contact angles of SPSf membranes

### 3.5. Fenton chemical stability

The Fenton test is used to evaluate chemical degradation caused by hydroxyl radicals and its effects on fuel cell performance. The weight losses resulting from the Fenton reaction of membranes with thicknesses of 50 μm, 100 μm, and 150 μm are shown in Figure 9. When the results after 24 hours are examined, it is seen that the lowest weight loss was obtained as 4.42% in the membrane with a thickness of 100 μm. The highest weight loss occurred as 23.03% in the membrane with a thickness of 50 μm after 168 hours.

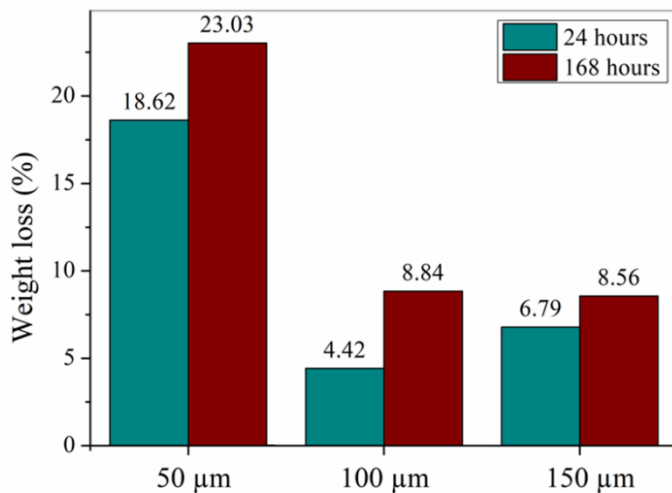


Figure 9. Fenton weight loss of SPSf membranes

### 3.6. Mechanical strength

The mechanical strength of the membranes is of critical importance for the performance, efficiency, and life of the fuel cell [42]. The values of elongation at break, Young's modulus, and tensile strength obtained by applying tensile tests for SPSf membranes with different thicknesses are presented in Table 3. The highest tensile stress value was 21.2 Mpa for the 100 μm membrane. The highest Young's modulus value was 764.7 Mpa for the 150 μm membrane. The elongation at break values of the membranes with thicknesses

of 50 μm, 100 μm, and 150 μm were 8.9%, 6.42%, and 5.54%, respectively. A regular decrease was observed in the elongation at break values with increasing thickness.

Table 3. Mechanical strength results of SPSf membranes

Samples	Tensile strength (MPa)	Young modulus (MPa)	Elongation at break (%)
50 μm	19.2	751.48	8.9
100 μm	21.2	713.44	6.42
150 μm	19.2	764.7	5.54

## 4. Conclusions

In this study, SPSf polymer-based membranes with 50 μm, 100 μm, and 150 μm thickness were fabricated, and their characteristic properties were investigated. The highest water uptake capacity and swelling ratio were obtained as 45.81% and 13.1% for 100 μm membranes, respectively. It was observed that the resistance value decreased with decreasing membrane thickness, and proton conductivity increased. The increase in temperature and acid in the measurement environment caused an increase in the proton conductivity value. The highest proton conductivity value was obtained as 0.1971 S/cm in 50 μm SPSf membrane at 65 °C and 1 mM HCl aqueous solution. As a result of contact angle analyses, it was observed that SPSf membranes of all thicknesses synthesized were hydrophilic. Chemical stability was positively affected by the increase in membrane thickness. The highest tensile strength value was obtained as 21.2 Mpa in the membrane with a thickness of 100 μm. A regular increase in elongation at break was observed with the decrease in membrane thickness.

## Acknowledgment

This study was supported by Gazi University Research Projects Coordination Unit (BAP) with project number of FGA-2023-7912 in the scope of Research Universities Support Program.

## Conflict of Interest Statement

The authors declare that there is no conflict of interest in the study.

## CRedit Author Statement

**İrem Tanış:** Writing-original draft, Visualization, Investigation, Conceptualization. **Turan Alp Arslan:** Writing-original draft, Visualization, Investigation. **Tolga Kocakulak:** Writing-original draft, Visualization, Investigation. **Gülşen Taşkın:** Writing – review & editing, Investigation, Methodology. **Tuğba Tabanlıgil Calam:** Writing – review & editing, Investigation, Conceptualization. **Hamit Solmaz:** Writing – review & editing, Supervision, Project administration, Methodology.

## References

- Deshmukh, M. K. G., Sameeruddin, M., Abdul, D., & Sattar, M. A. (2023). Renewable energy in the 21st century: A review. *Materials Today: Proceedings*, 80, 1756-1759.
- Xu, Y., & Zhao, F. (2023). Impact of energy depletion, human development, and income distribution on natural resource sustainability. *Resources Policy*, 83, 103531.
- Kocakulak, T., & Arslan, T. A. (2023). Investigation of the use of fuel cell hybrid systems for different purposes. *Engineering Perspective*, 3(1), 1-8.

4. Majeed, Y., Khan, M. U., Waseem, M., Zahid, U., Mahmood, F., Majeed, F., ... & Raza, A. (2023). Renewable energy as an alternative source for energy management in agriculture. *Energy Reports*, 10, 344-359.
5. Zahedi, R., Sadeghitabar, E., Khazaei, M., Faryadras, R., & Ahmadi, A. (2024). Potentiometry of wind, solar and geothermal energy resources and their future perspectives in Iran. *Environment, Development and Sustainability*, 1-27.
6. Awad, M., Said, A., Saad, M. H., Farouk, A., Mahmoud, M. M., Alshammari, M. S., ... & Omar, A. I. (2024). A review of water electrolysis for green hydrogen generation considering PV/wind/hybrid/hydropower/geothermal/tidal and wave/biogas energy systems, economic analysis, and its application. *Alexandria Engineering Journal*, 87, 213-239.
7. Aniakor, C. O. (2024). Mapping renewable energy technologies (solar, wind and geothermal) to the United Nations' Sustainable Development Goals (SDGs) to reveal and quantify synergies and tradeoffs. Available at SSRN: 10.2139/ssrn.4842618.
8. Van Der Linden, F., Pahon, E., Morando, S., & Bouquain, D. (2023). A review on the proton-exchange membrane fuel cell break-in physical principles, activation procedures, and characterization methods. *Journal of Power Sources*, 575, 233168.
9. Bodkhe, R. G., Shrivastava, R. L., Soni, V. K., & Chadge, R. B. (2023). A review of renewable hydrogen generation and proton exchange membrane fuel cell technology for sustainable energy development. *International Journal of Electrochemical Science*, 18(5), 100108.
10. Kumuk, B. (2019). A review of fuel cell types and applications. *Turkish Journal of Energy Policy*, 4(9), 1-9.
11. Ramasamy, P., Muruganatham, B., Rajasekaran, S., Babu, B. D., Ramkumar, R., Marthanda, A. V. A., & Mohan, S. (2024). A comprehensive review on different types of fuel cell and its applications. *Bulletin of Electrical Engineering and Informatics*, 13(2), 774-780.
12. Shuhayey, P., Martsinchyk, A., Martsinchyk, K., Szczeńniak, A., Szablowski, L., Dybiński, O., & Milewski, J. (2024). Model-based quantitative characterization of anode microstructure and its effect on the performance of molten carbonate fuel cell. *International Journal of Hydrogen Energy*, 52, 902-915.
13. Mancino, A. N., Menale, C., Vellucci, F., Pasquali, M., & Bubbico, R. PEM fuel cell applications in road transport. *Energies*, 16(17), 6129.
14. Maher, A. R., & Sadiq, A. B. (2013). PEM fuel cells: Fundamentals, modeling, and applications. Create Space Independent Publishing Platform, Washington.
15. Amani, B., & Zanj, A. (2023). Analysis of the effects of the gas diffusion layer properties on the effectiveness of baffled flow channels in improving proton exchange membrane fuel cells performance. *International Communications in Heat and Mass Transfer*, 140, 106558.
16. Zhou, S., Xie, G., Hu, H., & Ni, M. (2023). Simulation on water transportation in gas diffusion layer of a PEM fuel cell: Influence of non-uniform PTFE distribution. *International Journal of Hydrogen Energy*, 48(28), 10644-10658.
17. Zhang, G., Qu, Z., & Wang, Y. (2023). Proton exchange membrane fuel cell of integrated porous bipolar plate-gas diffusion layer structure: Entire morphology simulation. *eTransportation*, 17, 100250.
18. Lufano, F., Baglio, V., Staiti, P., Stassi, A., Aricò, A. S., & Antonucci, V. (2010). Investigation of sulfonated polysulfone membranes as electrolyte in a passive-mode direct methanol fuel cell mini-stack. *Journal of Power Sources*, 195(23), 7727-7733.
19. Zhang, Y., Zheng, L., Liu, B., Wang, H., & Shi, H. (2019). Sulfonated polysulfone proton exchange membrane influenced by a varied sulfonation degree for vanadium redox flow battery. *Journal of Membrane Science*, 584, 173-180.
20. Liu, J. G., Zhao, T. S., Liang, Z. X., & Chen, R. (2006). Effect of membrane thickness on the performance and efficiency of passive direct methanol fuel cells. *Journal of Power Sources*, 153(1), 61-67.
21. Kocakulak, T., Taşkın, G., Calam, T. T., Solmaz, H., Calam, A., Arslan, T. A., & Şahin, F. (2024). A new nanocomposite membrane based on sulfonated polysulfone boron nitride for proton exchange membrane fuel cells: Its fabrication and characterization. *Fuel*, 374, 132476.
22. Lufano, F., Gatto, I., Staiti, P., Antonucci, V., & Passalacqua, E. (2001). Sulfonated polysulfone ionomer membranes for fuel cells. *Solid State Ionics*, 145(1-4), 47-51.
23. Wang, G., Kang, J., Yang, S., Lu, M., & Wei, H. (2024). Influence of structure construction on water uptake, swelling, and oxidation stability of proton exchange membranes. *International Journal of Hydrogen Energy*, 50, 279-311.
24. Selim, A., Szijjártó, G. P., Románszki, L., & Tompos, A. (2022). Development of WO<sub>3</sub>-Nafion based membranes for enabling higher water retention at low humidity and enhancing PEMFC performance at intermediate temperature operation. *Polymers*, 14(12), 2492.
25. Chen, F., Dong, W., Lin, F., Ren, W., & Ma, X. (2021). Composite proton exchange membrane with balanced proton conductivity and swelling ratio improved by gradient-distributed POSS nanospheres. *Composites Communications*, 24, 100676.
26. Li, J., Cui, N., Liu, D., Zhao, Z., Yang, F., Zhong, J., & Pang, J. (2024). SPEEK-co-PEK-x proton exchange membranes with controllable sulfonation degree for proton exchange membrane fuel cells. *International Journal of Hydrogen Energy*, 50, 606-617.
27. Zhang, Y., Zhang, A., He, H., Fan, Y., Li, Y., Wang, S., & Li, S. (2024). Fabrication of an ultra-thin and ordered SPEEK proton exchange membrane by a Langmuir-Blodgett self-assembly process. *Journal of Membrane Science*, 690, 122196.
28. Peighambari, S. J., Rowshanzamir, S., & Amjadi, M. (2010). Review of the proton exchange membranes for fuel cell applications. *International Journal of Hydrogen Energy*, 35(17), 9349-9384.
29. Lvovich, V. F. (2012). Impedance spectroscopy: Applications to electrochemical and dielectric phenomena. John Wiley & Sons.
30. Karpenko, L. V., Demina, O. A., Dvorkina, G. A., Parshikov, S. B., Larchet, C., Auclair, B., & Berezina, N. P. (2001). Comparative study of methods used for the determination of electroconductivity of ion-exchange membranes. *Russian Journal of Electrochemistry*, 37(3), 287-293.
31. Sistat, P., Kozmai, A., Pismenskaya, N., Larchet, C., Pourcelly, G., & Nikonenko, V. (2008). Low-frequency impedance of an ion-exchange membrane system. *Electrochimica Acta*, 53(22), 6380-6390.
32. Zhang, Y., Zhu, C., Zhang, J., & Liu, Y. (2024). Negative impact of poly(acrylic acid) on proton conductivity of electrospun catalyst layers. *Applied Energy*, 357, 122511.
33. Ng, W. W., San Thiam, H., Pang, Y. L., Lim, Y. S., Wong, J., & Saw, L. H. (2023). Self-sustainable, self-healable sulfonated graphene oxide incorporated nafion/poly(vinyl alcohol) proton exchange membrane for direct methanol fuel cell applications. *Journal of Environmental Chemical Engineering*, 11(6), 111151.
34. Bormashenko, E. Y. (2013). Wetting of real surfaces. Walter de Gruyter GmbH, Berlin.

35. Cosgrove, T. (2005). *Colloid science (Principles, methods and applications)*. Wiley-Blackwell Publishing Ltd., Oxford.
36. Sigwadi, R., Dhlamini, M. S., Mokrani, T., & Nemavhola, F. (2019). Enhancing the mechanical properties of zirconia/Nafion® nanocomposite membrane through carbon nanotubes for fuel cell application. *Heliyon*, 5(7), e02112.
37. Inaba, M., Kinumoto, T., Kiriake, M., Umebayashi, R., Tasaka, A., & Ogumi, Z. (2006). Gas crossover and membrane degradation in polymer electrolyte fuel cells. *Electrochimica Acta*, 51(26), 5746-5753.
38. Cheng, X., Zhang, J., Tang, Y., Song, C., Shen, J., Song, D., & Zhang, J. (2007). Hydrogen crossover in high-temperature PEM fuel cells. *Journal of Power Sources*, 167(1), 25-31.
39. Oh, S., Kim, J., Lee, D., & Park, K. (2018). Variation of hydrogen peroxide concentration during fenton reaction for test the membrane durability of PEMFC. *Korean Chemical Engineering Research*, 56(3), 315-319.
40. Dafalla, A. M., & Jiang, F. (2018). Stresses and their impacts on proton exchange membrane fuel cells: A review. *International Journal of Hydrogen Energy*, 43(4), 2327-2348.
41. Liu, W., Luo, N., Li, P., Yang, X., Dai, Z., Song, S., ... & Zhang, H. (2020). New sulfonated poly(ether ether ketone) composite membrane with the spherical bell-typed superabsorbent microspheres: Excellent proton conductivity and water retention properties at low humidity. *Journal of Power Sources*, 452, 227823.
42. Wallnöfer-Ogris, E., Poimer, F., Köll, R., Macherhammer, M. G., & Trattner, A. (2024). Main degradation mechanisms of polymer electrolyte membrane fuel cell stacks—Mechanisms, influencing factors, consequences, and mitigation strategies. *International Journal of Hydrogen Energy*, 50, 1159-1182.